Published in final edited form as:
Biochem Pharmacol. 2013 October 1; 86(7): 896–903. doi:10.1016/j.bcp.2013.08.002.

MLK3 is a direct target of biochanin A, which plays a role in solar UV-induced COX-2 expression in human keratinocytes

Tae-Gyu Lim[a,b,c], **Jong-Eun Kim**[a,b,c], **Sung Keun Jung**[a,b,d], **Yan Li**[a], **Ann M. Bode**[a], **Jun-Seong Park**[e], **Myeong Hun Yeom**[e], **Zigang Dong**[a,*], and **Ki Won Lee**[b,c,*]

[a] The Hormel Institute, University of Minnesota, 801 16th Avenue NE, Austin, MN, 55912, USA

[b] Advanced Institutes of Convergence Technology, Seoul National University, Suwon, 443-270, Republic of Korea

[c] WCU Biomodulation Major, Department of Agricultural Biotechnology and Center for Food and Bioconvergence, Seoul National University, Seoul, 151-921, Republic of Korea

[d] Division of Metabolism and Functionality Research, Korea Food Research Institute, Seongnam, Republic of Korea

[e] Skin Research Institute, Amorepacific Corporation R&D Center, Yongin-si, Gyeonggi-do, 341-1, Republic of Korea

Abstract

Solar UV (sUV) is an important environmental carcinogen. Recent studies have shown that sUV is associated with numerous human skin disorders, such as wrinkle formation and inflammation. In this study, we found that the isoflavone, biochanin A, inhibited the expression of sUV-induced COX-2, which is a well-characterized sUV-induced enzyme, in both human HaCaT keratinocytes and JB6 P+ mouse skin epidermal cells. Several studies have demonstrated the beneficial effects of biochanin A. However, its direct molecular target is unknown. We found that biochanin A inhibited sUV-induced phosphorylation of MKK4/JNK/c-Jun and MKK3/6/p38/MSK1. Mixed-lineage kinase 3 (MLK3) is an upstream kinase of MKK4 and MKK3/6. Thus, we evaluated the effect of biochanin A on MLK3. We found that sUV-induced MLK3 phosphorylation was not affected, whereas MLK3 kinase activity was significantly suppressed by biochanin A. Furthermore, direct binding of biochanin A in the MLK3 ATP-binding pocket was detected using pull-down assays. Computer modeling supported our observation that MLK3 is a novel target of biochanin A. These results suggest that biochanin A exerts chemopreventive effects by suppressing sUV-induced COX-2 expression mediated through MLK3 inhibition.

Keywords

Biochanin A; Cyclooxygenase-2; Mixed-lineage kinase 3; Solar UV

* Corresponding authors. zgdong@hi.umn.edu (Z. Dong), kiwon@snu.ac.kr (K.W. Lee)..

1. Introduction

Human skin is constantly exposed to various environmental factors, such as solar UV (sUV). Many previous studies have reported that repetitive exposure of skin to sUV causes physiological changes such as sunburn [1], wrinkle formation [2], and inflammation [3]. sUV comprises three subtypes, UVA (320– 400 nm), UVB (280–320 nm), and UVC (200–280 nm). UVC is blocked by the ozone layer, whereas human skin is exposed to UVA and UVB. sUV comprises approximately 95% UVA and 5% UVB. Accordingly, sUV is a suitable model for studies of physiological skin conditions.

Chronic inflammation is closely associated with several diseases, including cancer [4,5]. Thus, suppression of inflammation may be applicable as an anticancer strategy. Cyclooxygenases (COXs) are the rate-limiting enzymes for prostaglandin production from arachidonic acid and have two isoforms, COX-1 and COX-2. COX-1 is constitutively expressed, whereas COX-2 is an inducible isoform [6], which plays a critical role in carcinogenesis. Aberrant expression of COX-2 promotes cellular processes, including proliferation, angiogenesis, and differentiation [7,8]. In the skin, COX-2 is associated with skin homeostasis, but overexpression of COX-2 can result in pre-neoplastic skin phenotypes [9,10].

Previous studies indicated that COX-2 expression is regulated by inflammatory signaling pathways, such as the mitogen-activated protein kinase (MAPK) family of signaling proteins [11–13]. MAPK kinase kinase (MAP3K) phosphorylates MAP2K and subsequently activates MAPK [14]. Among the MAP3K family, mixed-lineage kinase 3 (MLK3) is well characterized and involved in many inflammatory signaling cascades, as well as cancer [15–18]. Tibbles et al. reported that MLK3 directly phosphorylates SEK1 and MKK3/6, and subsequently activates the JNKs and p38 signaling pathways, respectively [19]. Additionally, Gallo and Johnson demonstrated that MLK3 regulates the JNKs and p38 signaling pathways [20].

Isoflavones are major components of soy. Recent studies reported that isoflavones exert chemopreventive and anticancer effects [21–24], primarily due to their antioxidative activities [25,26]. However, reports have also suggested that isoflavones have phyto-estrogenic effects [27] and function as small molecule inhibitors in cancer [28]. Biochanin A (Fig. 1A, *upper*) is an isoflavone found in red clover. Although biochanin A is known to have beneficial effects, its direct molecular target remains unknown [29–31].

Overall, we found that biochanin A inhibited sUV-induced COX-2 expression by directly targeting MLK3. Based on kinase assay data, we confirmed that biochaninA suppressed MLK3 kinase activity, and pull-down assays revealed an interaction between biochanin A and MLK3. Because several studies have indicated that MLK3 regulates the JNKs and p38 signaling pathways by phosphorylating MKK4 and MKK3/6 [17,19,20,32], we hypothesized that attenuation of the MKK4/JNK/c-Jun and MKK3/6/p38/ MSK signaling pathways is caused by direct inhibition of MLK3 by biochanin A.

2. Materials and methods

2.1. Materials

Biochanin A, phosphorylated MLK3 (Thr^{277}/Ser^{281}) and the β-actin antibody were purchased from Sigma–Aldrich (St. Louis, MO). The COX-2 primary antibody was obtained from Cayman Chemical (Ann Arbor, MI), and primary antibodies recognizing phosphorylated p38 (Tyr^{180}/Tyr^{182}), total p38, phosphorylated MEK (Ser$^{217/221}$), total MEK, phosphorylated SEK1/MKK4 (MKK4, Ser^{257}/Thr^{261}), phosphorylated MKK3 (Ser^{189})/6 (Ser^{207}), total MKK3, phosphorylated c-Jun (Ser^{63}), total c-Jun, phosphorylated MSK (Ser^{376}), total MSK1, phosphorylated p90RSK (Thr^{359}/Ser^{363}), total p90RSK, phosphorylated MLK3, and total MLK3 were obtained from Cell Signaling Biotechnology (Beverly, MA). Antibodies to detect phosphorylated ERKs (Tyr^{204}), total ERKs, total MKK4, phosphorylated JNKs, and total JNKs were purchased from Santa Cruz Biotechnology (Santa Cruz, CA). G418 sulfate was obtained from Mediatech (Herndon, VA) and fetal bovine serum (FBS) was purchased from Gemini Bio-Products (West Sacramento, CA). CNBr-Sepharose 4B beads, [γ-^{32}P]-ATP, and the chemiluminescence detection kit were obtained from GE Health-care (Piscataway, NJ). Dulbecco's Modified Eagle's Medium (DMEM) was purchased from Hyclone (San Diego, CA). The protein assay kit was obtained from Bio-Rad Laboratories (Hercules, CA).

2.2. Cell culture

Human HaCaT cells were cultured in DMEM supplemented with 10% FBS and 0.1% penicillin/streptomycin at 37 °C in a humidified atmosphere of 5% CO_2. The JB6 P+ cell line was cultured in MEM supplemented with 5% FBS and 0.1% penicillin/streptomycin at 37 °C in a humidified atmosphere of 5% CO_2.

2.3. Cell cytotoxicity

To evaluate the cytotoxicity of biochanin A, HaCaT and JB6 P+ cells were cultured to confluence in 96-well plates. Then, the cells were treated with biochanin A for 24 h. Cell viability was analyzed using Cell Titer96 Aqueous One Solution (Promega, Madison, WI) by incubating with 20 μl of MTS solution for 1 h at 37 °C in a 5% CO_2 incubator. The absorbance was read at 492 nm.

2.4. sUV irradiation systems

The source of solar UV was UVA-340 lamps purchased from QLab Corporation (Cleveland, OH). The UVA-340 lamps provide the best possible simulation of sunlight in the critical short wavelength region from 365 nm down to the solar cutoff of 295 nm with a peak emission of 340 nm. The percentage of UVA and UVB of UVA-340 lamps was measured by a UV meter and was 94.5% and 5.5% respectively. The dose of sUV used in this study was 90 kJ/m^2.

2.5. Western blot analysis

HaCaT cells were cultured to 100% confluency and starved in serum-free DMEM for 24 h to eliminate FBS-mediated activation of protein kinases. Biochanin A was added to cells at

various concentrations (0, 10, 20 or 40 μM). After 1 h of biochanin A treatment, the cells were exposed to sUV (90 kJ/m^2). The cells were harvested using lysis buffer [10 mM Tris (pH 7.5), 150 mM NaCl, 5 mM ethylene diamine tetraacetic acid (EDTA), 1% Triton X-100, 1 mM dithiothreitol (DTT), 0.1 mM phenylmethylsulfonyl fluoride (PMSF), 10% glycerol and protease inhibitor cocktail tablet]. Equal amounts of proteins were separated on 10% SDS-polyacrylamide gels. Subsequently, the proteins were transferred to Immobilon P membranes (Millipore, Billerica, MA). The membranes were blocked with 5% fat-free milk for 1 h, and incubated with specific primary antibodies at 4 °C overnight. Next, the proteins were hybridized with HRP-conjugated secondary antibodies and detected using a chemiluminescence detection kit (GE Healthcare, Pittsburgh, PA). The quantification of protein expression and phosphorylation in each band was analyzed using the Image J software program.

2.6. Luciferase assay for AP-1 transactivation

HaCaT cells were stably transfected with an AP-1 luciferase reporter plasmid. The cells were maintained in 10% FBS-DMEM containing 200 μg/ml of G418. After starvation for 24 h in serum-free DMEM, biochanin A was added at various concentrations (0, 10, 20 and 40 μM) for 1 h before sUV irradiation. At 1 h after sUV exposure, the cells were harvested using lysis buffer [0.1 M potassium phosphate buffer (pH 7.8), 1% Triton X-100, 1 mM DTT and 2 mM EDTA]. Luciferase activity was evaluated using a luminometer (Luminoskan Ascent; Thermo Electron, Helsinki, Finland). The results are shown as a comparison to untreated control cells exposed to sUV irradiation (100%).

2.7. MLK3, TAK1, and JNK1 kinase assays

Kinase activities of MLK3, TAK1, and JNK1 were measured according to the manufacturer's instructions (Millipore, Bedford, MA). Briefly, the specific enzymes were incubated with biochanin A (0, 10, 20 or 40 μM) at 30 °C for 20 min in assay buffer [20 mM MOPS (pH 7.2), 25 mM β-glycerol phosphate, 5 mM EGTA, 1 mM sodium orthovanadate and 1 mM DTT]. Myelin basic protein (MBP) and a [γ-^{32}P]-ATP solution were added to the mixture and incubated at 30 °C for 20 min in magnesium acetate–ATP cocktail buffer (Upstate Biotechnology Inc., Lake Placid, NY). Each sample (15 μl) was transferred onto p81 paper and the paper was then washed with 0.75% phosphoric acid and acetone for 5 min. The specific kinase activities were estimated using a scintillation counter.

2.8. KinaseProfiler™ service

KinaseProfiler™ analysis was conducted by the Kinase Profiler™ service (MERCK Millipore) according to the protocols detailed at http://www.millipore.com/techpublications/tech1/pf3036.

2.9. Preparation of biochanin A-CNBr-activated Sepharose 4B beads

CNBr-activated Sepharose 4B freeze-dried powder (GE Health-care, Pittsburgh, PA) was suspended in 30 mL of 1 mM HCl. Biochanin A (2 mg) was added to activated Sepharose 4B in coupling buffer (0.1 M $NaHCO_3$ [pH 8.3] and 0.5 M NaCl) and rotated at 4 °C overnight. The mixture was transferred to 0.1 M Tris–HCl buffer (pH 8.0) and rotated again

at 4 °C overnight. Uncoupled biochanin A was removed by washing with 0.1 M acetate buffer (pH 4.0) and 0.1 M Tris–HCl buffer (pH 8.0) containing 0.5 M NaCl.

2.10. Cell-based pull-down assays

HaCaT cell lysate (500 μg) was mixed with biochanin A–Sepharose 4B beads (100 μL) or Sepharose 4B beads alone and incubated in reaction buffer (50 mM Tris [pH 7.5], 5 mM EDTA, 150 mM NaCl, 1 mM DTT, 0.01% Nonidet P-40, 2 μg/ml bovine serum albumin, 0.02 μM PMSF, and 1 × protease inhibitor mixture) overnight. Then the mixture was washed with washing buffer (50 mM Tris [pH 7.5], 5 mM EDTA, 150 mM NaCl, 1 mM DTT, 0.01% Nonidet P-40, and 0.02 mM PMSF) and the proteins were detected by immunoblotting. Briefly, the mixture was separated on 10% SDS-polyacrylamide gels and the proteins were transferred to Immobilon P membranes (Millipore, Billerica, MA). The membranes were blocked with 5% fat-free milk for 1 h, and incubated with a specific MLK3 antibody at 4 °C overnight. Next, the proteins were hybridized with an HRP-conjugated secondary antibody and detected using a chemiluminescence detection kit (GE Healthcare, Pittsburgh, PA).

2.11. Computer modeling

The MLK3 (MAP3K11) structure was modeled by comparative modeling based on the MLK1 (MAP3K9) crystal structure. MLK1 and MLK3 have a high sequence similarity (77%). The MLK1 crystal structure was obtained from the RCSB Protein Data Bank (PDB entry: 3DTC). Alignment of the MLK1 and MLK3 sequences was performed using BLAST and edited in Prime v3.0. The secondary structure of MLK3 was predicted using SSpro. The 3-D structure of MLK3 was built using Prime v3.0 and the loops in the binding site were refined and minimized. Glide v5.7 was used for the docking of MLK3 and biochanin A. Biochanin A was prepared using LigPrep v2.5, and then assigned AMSOL partial atom charges. Flexible docking was performed in the extra precision (XP) mode. The number of poses per ligand was set to 10 in the post-docking minimization. The default settings were used for all other parameters.

3. Results

3.1. Biochanin A suppresses sUV-induced COX-2 expression and AP-1 transactivation in HaCaT cells

Aberrant expression of COX-2 promotes skin inflammation [5,9,10]. We examined the effect of biochanin A on sUV-induced COX-2 expression in HaCaT and JB6 P+ cells. The concentrations of biochanin in the current study did not affect the viability of HaCaT or JB6 P+ cells (Fig. 1A, lower). In agreement with a previous study [33], sUV exposure increased COX-2 expression, and pretreatment with biochanin A (10, 20 or 40 μM) reduced sUV-induced COX-2 expression (Fig. 1B, C). AP-1 is a transcription factor for several inflammatory cytokines and *cox-2* is a target gene of AP-1 [34]. Thus, we evaluated the effect of biochanin A on sUV-induced AP-1 transactivation using HaCaT cells stably transfected with a luciferase reporter plasmid bearing AP-1. We found that biochanin A (10, 20 and 40 μM) significantly inhibited sUV-induced AP-1 transactivation (Fig. 1D). Thus, we

concluded that biochanin A attenuated sUV-induced COX-2 expression at the transcriptional level.

3.2. Biochanin A inhibits sUV-induced MKK4/JNKs/c-Jun and MKK3/6/ p38/MSK, but not the MEK/ERKs/p90RSK, signaling pathway

Environmental sUV irradiation increases MAPK signaling [35] and subsequently induces COX-2 expression [36]. Thus, we evaluated the effect of biochanin A on the sUV-induced MAPK signaling pathway. While sUV exposure induced all MAPK signaling pathways (Fig. 2), pretreatment with biochanin A (0, 10, 20 and 40 μM) inhibited MKK4/JNKs/c-Jun and MKK3/6/p38/MSK phosphorylation (Fig. 2A, B). However, MEK/ERKs/p90RSK (Fig. 2C) signaling was not affected by biochanin A. These results suggest that the biochanin A target is upstream of MKK4/JNKs/c-Jun and MKK3/ 6/p38/MSK.

3.3. MLK3 is a direct target of biochanin A in an in vitro sUV model

Because biochanin A inhibited MKK4/JNKs/c-Jun and MKK3/6/ p38/MSK signaling (Fig. 2), we investigated its effect on MLK3 phosphorylation. Several reports have shown that MLK3 plays a role in the JNKs and p38 signaling pathways by directly phosphorylating MKK4 and MKK3/6 [19,20] and is associated with inflammation [37,38]. MLK3 was highly phosphorylated after sUV exposure; however, this phosphorylation was not inhibited by biochanin A (10, 20 and 40 μM) (Fig. 3A). Next, we evaluated the effect of biochanin A on MLK3 kinase activity *in vitro*. The *in vitro* kinase assay showed that biochanin A (10, 20 or 40 μM) directly inhibited MLK3 kinase activity (Fig. 3B). To investigate whether biochanin A selectively suppresses MLK3 kinase activity, we examined its effect on TAK1 and JNK1 kinase activities using an *in vitro* kinase assay. Results indicated that the kinase activity of TAK1 (Fig. 3C) or JNK1 (Fig. 3D) was not affected by biochanin A (10, 20 or 40 μM). The results of MERCK Millipore's KinaseProfiler™ service indicated that biochanin A did not inhibit any additional kinase tested (including ASK1, TAK1, TAO1, TAO2 and c-Raf) (Table 1). Overall, these results suggest that biochanin A selectively inhibits MLK3 kinase activity.

3.4. Biochanin A directly binds to the MLK3 ATP-binding pocket

In order for biochanin A to suppress kinase activity, it should bind to MLK3 directly. Thus, we examined MLK3 and biochanin A binding using *in vitro* and *ex vivo* binding assays. We found that biochanin A binds the MLK3 protein both *in vitro* (Fig. 4A) and in a cell lysate (Fig. 4B). If biochanin A binds to the MLK3 ATP-binding pocket, the binding should be reduced by the addition of ATP and results indicated that the binding between biochanin A and MLK3 was reduced by ATP in a dose-dependent manner (Fig. 4C). Based on these results, we conclude that biochanin A binds directly to the ATP-binding pocket of MLK3. Computer modeling provided supporting evidence that biochanin A occupies the ATP-binding pocket of MLK3 (Fig. 5, *left*) and suggested that it forms hydrogen bonds with Ala^{83} and Arg^{90} (Fig. 5, *right*).

4. Discussion

Biochanin A is an isoflavone and a major constituent of red clover [39,40]. Although many groups have demonstrated the beneficial effects of biochanin A, including an anti-proliferation effect on squamous cell carcinoma [41], anti-inflammatory, immune suppressive [42], and LDL cholesterol-lowering effects [43], the direct mechanisms of action of biochanin A are not fully understood. Several proteins and signaling pathways have been suggested to mediate the mechanism of biochanin A's actions. Johnson et al. reported that biochanin A inhibited cell proliferation by suppressing ERKs and Akt phosphorylation [41]. However, to the best of our knowledge, no one has reported that MLK3 is a direct target of biochanin A.

In the present study, biochanin A inhibited sUV-induced COX-2 expression by targeting MLK3. MLK3 is an MAP3K protein, which mediates JNKs and p38 signaling pathways by phosphorylating MKK4 and MKK3/6, respectively [19,20]. Some studies have reported that MLK3 is associated with cancer development [17,44] and metabolic stress [16]. In the present study, biochanin A inhibited sUV-induced MKK4/JNKs/c-Jun and MKK3/6/p38/MSK, but not MEK/ERKs/p90RSK signaling. Furthermore, we found that biochanin A reduces MLK3 kinase activity and directly binds in the MLK3 ATP-binding pocket. In contrast, biochanin A did not significantly affect TAK1 and JNK1 kinase activities. This suggests that biochanin A selectively inhibits MLK3. However, several studies have also reported the regulation of isoflavones on NF-kB signaling [45,46]. Thus, to confirm whether biochanin A affects sUV-induced NF-kB activation, further study is necessary for supporting the effect of biochanin A on COX-2 expression.

Recent studies have shown that the MEK/ERKs signaling pathway is also regulated by MLK3 [32,47,48]. However, in the present study, biochanin A suppressed MLK3 kinase activity, whereas the sUV-induced MEK/ERKs/p90RSK signaling pathway was unaffected. Thus, we concluded that MLK3 regulates MKK4/ JNKs/c-Jun and MKK3/6/p38/MSK, but not MEK/ERKs/p90RSK, signaling in a sUV-induced HaCaT cell-COX-2 expression model. To confirm this hypothesis, further studies using MLK3 knockdown or knockout models are required. Because the current study is the first to identify a direct target of biochanin A, additional *in vivo* and clinical studies will be helpful for explaining these findings.

Previous studies have shown that isoflavones exhibit phytoestrogenic activity [27]. However, Shemesh, et al. found that biochanin A did not have a high binding affinity to the estrogen receptor *in vivo* [49]. Thus, the effects of biochanin A on sUV-induced COX-2 expression are not likely due to phyto-estrogenic activity. Although several groups have reported the biological activities of biochanin A, including apoptotic [31], anti-hyperglycemic [50] and pytotoxic [51] effects, a direct target of biochanin A was not identified.

These results indicate that biochanin A directly suppresses MLK3 kinase activity by binding to its ATP pocket in HaCaT cells. Subsequent sUV-induced COX-2 expression was decreased, which resulted from suppression of MKK/JNKs/c-Jun and MKK3/6/p38/ MSK

signaling pathway. This study demonstrates a potential target of sUV-induced skin inflammation. Because a previous study indicated that biochanin A inhibits the NF-κB signaling pathway [52], the effect of biochanin A on sUV-induced NF-κB pathway should be investigated. To expand on the importance of this finding, *in vivo* or clinical studies will be required.

Acknowledgments

This work was supported by The Hormel Foundation and National Institutes of Health grants CA166011, CA172457, CA120388, R37 CA081064 and NIESH grant ES 016548; the National Research Foundation of Korea (NRF) grant funded by the Korean government (MEST) (No. 2010-0029233), Interrelated Development Program (R-0000451) of Inter-Economic Regions, Ministry for Knowledge Economy and High Value-added Food Technology Development Program (311035-3), Ministry for Food, Agriculture, Forestry and Fisheries, Republic of Korea.

References

1. Heenen M, Giacomoni PU, Golstein P. Individual variations in the correlation between erythemal threshold, UV-induced DNA damage and sun-burn cell formation. Journal of Photochemistry and Photobiology. 2001; 63:84–7.
2. Kawada S, Ohtani M, Ishii N. Increased oxygen tension attenuates acute ultraviolet-B-induced skin angiogenesis and wrinkle formation. American Journal of Physiology. 2010; 299:R694–701. [PubMed: 20504908]
3. Van Nguyen H, Di Girolamo N, Jackson N, Hampartzoumian T, Bullpitt P, Tedla N, et al. Ultraviolet radiation-induced cytokines promote mast cell accumulation and matrix metalloproteinase production: potential role in cutaneous lupus erythematosus. Scandinavian Journal of Rheumatology. 2011; 40:197–204. [PubMed: 21247265]
4. Wilgus TA, Koki AT, Zweifel BS, Kusewitt DF, Rubal PA, Oberyszyn TM. Inhibition of cutaneous ultraviolet light B-mediated inflammation and tumor formation with topical celecoxib treatment. Molecular Carcinogenesis. 2003; 38:49–58. [PubMed: 14502644]
5. Rundhaug JE, Mikulec C, Pavone A, Fischer SM. A role for cyclooxygenase-2 in ultraviolet light-induced skin carcinogenesis. Molecular Carcinogenesis. 2007; 46:692–8. [PubMed: 17443745]
6. Smith WL, DeWitt DL, Garavito RM. Cyclooxygenases: structural, cellular, and molecular biology. Annual Review of Biochemistry. 2000; 69:145–82.
7. Vane JR, Bakhle YS, Botting RM. Cyclooxygenases 1 and 2. Annual Review of Pharmacology and Toxicology. 1998; 38:97–120.
8. Dubois RN, Abramson SB, Crofford L, Gupta RA, Simon LS, Van De Putte LB, et al. Cyclooxygenase in biology and disease. FASEB Journal Official Publication of the Federation of American Societies for Experimental Biology. 1998; 12:1063–73. [PubMed: 9737710]
9. Buckman SY, Gresham A, Hale P, Hruza G, Anast J, Masferrer J, et al. COX-2 expression is induced by UVB exposure in human skin: implications for the development of skin cancer. Carcinogenesis. 1998; 19:723–9. [PubMed: 9635856]
10. Fosslien E. Molecular pathology of cyclooxygenase-2 in neoplasia. Annals of clinical and Laboratory Science. 2000; 30:3–21. [PubMed: 10678579]
11. Kumar Senthil A, Bansal K, Holla S, Verma-Kumar S, Sharma P, Balaji KN. ESAT-6 induced COX-2 expression involves coordinated interplay between PI3K and MAPK signaling. Molecular Immunology. 2012; 49:655–63. [PubMed: 22154837]
12. Keum YS, Kim HG, Bode AM, Surh YJ, Dong Z. UVB-induced COX-2 expression requires histone H3 phosphorylation at Ser10 and Ser28. Oncogene. 2013
13. Woo JG, Park SY, Lim JC, Joo MJ, Kim HR, Sohn UD. Acid-induced COX-2 expression and prostaglandin E2 production via activation of ERK1/2 and p38 MAPK in cultured feline esophageal smooth muscle cells. Archives of Pharmacal Research. 2011; 34:2131–40. [PubMed: 22210040]

14. Winter-Vann AM, Johnson GL. Integrated activation of MAP3Ks balances cell fate in response to stress. Journal of Cellular Biochemistry. 2007; 102:848–58. [PubMed: 17786929]
15. Hong HY, Kim BC. Mixed lineage kinase 3 connects reactive oxygen species to c-Jun NH2-terminal kinase-induced mitochondrial apoptosis in genipin-treated PC3 human prostate cancer cells. Biochemical and Biophysical Research Communications. 2007; 362:307–12. [PubMed: 17707342]
16. Jaeschke A, Davis RJ. Metabolic stress signaling mediated by mixed-lineage kinases. Molecular Cell. 2007; 27:498–508. [PubMed: 17679097]
17. Kim KY, Kim BC, Xu Z, Kim SJ. Mixed lineage kinase 3 (MLK3)-activated p38 MAP kinase mediates transforming growth factor-beta-induced apoptosis in hepatoma cells. The Journal of Biological Chemistry. 2004; 279:29478–84. [PubMed: 15069087]
18. Mishra P, Senthivinayagam S, Rangasamy V, Sondarva G, Rana B. Mixed lineage kinase-3/JNK1 axis promotes migration of human gastric cancer cells following gastrin stimulation. Molecular Endocrinology (Baltimore MD). 2010; 24:598–607.
19. Tibbles LA, Ing YL, Kiefer F, Chan J, Iscove N, Woodgett JR, et al. MLK-3 activates the SAPK/JNK and p38/RK pathways via SEK1 and MKK3/6. The EMBO journal. 1996; 15:7026–35. [PubMed: 9003778]
20. Gallo KA, Johnson GL. Mixed-lineage kinase control of JNK and p38 MAPK pathways. Nature Reviews. 2002; 3:663–72.
21. Akaza H. Prostate cancer chemoprevention by soy isoflavones: Role of intestinal bacteria as the “second human genome”. Cancer Science. 2012
22. Bronikowska J, Szliszka E, Czuba ZP, Zwolinski D, Szmydki D, Krol W. The combination of TRAIL and isoflavones enhances apoptosis in cancer cells. Molecules (Basel Switzerland). 2010; 15:2000–15.
23. Brown NM, Belles CA, Lindley SL, Zimmer-Nechemias LD, Zhao X, Witte DP, et al. The chemopreventive action of equol enantiomers in a chemically induced animal model of breast cancer. Carcinogenesis. 2010; 31:886–93. [PubMed: 20110282]
24. Szliszka E, Czuba ZP, Mertas A, Paradysz A, Krol W. The dietary isoflavone biochanin-A sensitizes prostate cancer cells to TRAIL-induced apoptosis. Urologic Oncology. 2013
25. Boadi WY, Iyere PA, Adunyah SE. In vitro exposure to quercetin and genistein alters lipid peroxides and prevents the loss of glutathione in human progenitor mononuclear (U937) cells. Journal of Applied Toxicology. 2005; 25:82–8. [PubMed: 15669027]
26. Mitchell JH, Gardner PT, McPhail DB, Morrice PC, Collins AR, Duthie GG. Antioxidant efficacy of phytoestrogens in chemical and biological model systems. Archives of Biochemistry and Biophysics. 1998; 360:142–8. [PubMed: 9826439]
27. Occhiuto F, Pasquale RD, Guglielmo G, Palumbo DR, Zangla G, Samperi S, et al. Effects of phytoestrogenic isoflavones from red clover (Trifolium pratense L.) on experimental osteoporosis. Phytotherapy Research. 2007; 21:130–4. [PubMed: 17117453]
28. Lee DE, Lee KW, Song NR, Seo SK, Heo YS, Kang NJ, et al. 7,3′,4′-Trihydroxyisoflavone inhibits epidermal growth factor-induced proliferation and transformation of JB6 P+ mouse epidermal cells by suppressing cyclin-dependent kinases and phosphatidylinositol 3-kinase. Journal of Biological Chemistry. 2010; 285:21458–66. [PubMed: 20444693]
29. Lin VC, Ding HY, Tsai PC, Wu JY, Lu YH, Chang TS. In vitro and in vivo melanogenesis inhibition by biochanin A from Trifolium pratense. Bioscience Biotechnology and Biochemistry. 2011; 75:914–8.
30. Qiu L, Lin B, Lin Z, Lin Y, Lin M, Yang X. Biochanin A ameliorates the cytokine secretion profile of lipopolysaccharide-stimulated macrophages by a PPAR-gamma-dependent pathway. Molecular Medicine Reports. 2012; 5:217–22. [PubMed: 21946955]
31. Seo YJ, Kim BS, Chun SY, Park YK, Kang KS, Kwon TG. Apoptotic effects of genistein, biochanin-A and apigenin on LNCaP and PC-3 cells by p21 through transcriptional inhibition of polo-like kinase-1. Journal of Korean Medical Science. 2011; 26:1489–94. [PubMed: 22065906]
32. Chadee DN, Kyriakis JM. MLK3 is required for mitogen activation of B-Raf, ERK and cell proliferation. Nature Cell Biology. 2004; 6:770–6.

33. Lam AN, Demasi M, James MJ, Husband AJ, Walker C. Effect of red clover isoflavones on cox-2 activity in murine and human monocyte/macrophage cells. Nutrition and Cancer. 2004; 49:89–93. [PubMed: 15456640]
34. Bode AM, Dong Z. Signal transduction pathways in cancer development and as targets for cancer prevention. Progress in Nucleic Acid Research and Molecular Biology. 2005; 79:237–97. [PubMed: 16096030]
35. Li S, Zhu F, Zykova T, Kim MO, Cho YY, Bode AM, et al. T-LAK cell-originated protein kinase (TOPK) phosphorylation of MKP1 protein prevents solar ultra-violet light-induced inflammation through inhibition of the p38 protein signaling pathway. Journal of Biological Chemistry. 2011; 286:29601–09. [PubMed: 21715333]
36. Chang KC, Wang Y, Oh IG, Jenkins S, Freedman LP, Thompson CC, et al. Estrogen receptor beta is a novel therapeutic target for photoaging. Molecular Pharmacology. 2010; 77:744–50. [PubMed: 20110405]
37. Handley ME, Rasaiyaah J, Chain BM, Katz DR. Mixed lineage kinases (MLKs): a role in dendritic cells, inflammation and immunity. International Journal of Experimental Pathology. 2007; 88:111–26. [PubMed: 17408454]
38. Wang MJ, Huang HY, Chen WF, Chang HF, Kuo JS. Glycogen synthase kinase-3beta inactivation inhibits tumor necrosis factor-alpha production in micro-glia by modulating nuclear factor kappaB and MLK3/JNK signaling cascades. Journal of Neuroinflammation. 2010; 7:99. [PubMed: 21194439]
39. Delmonte P, Perry J, Rader JI. Determination of isoflavones in dietary supplements containing soy, red clover and kudzu: extraction followed by basic or acid hydrolysis. Journal of Chromatography A. 2006; 1107:59–69. [PubMed: 16413562]
40. Tsao R, Papadopoulos Y, Yang R, Young JC, McRae K. Isoflavone profiles of red clovers and their distribution in different parts harvested at different growing stages. Journal of Agricultural and Food Chemistry. 2006; 54:5797–805. [PubMed: 16881680]
41. Johnson TL, Lai MB, Lai JC, Bhushan A. Inhibition of cell proliferation and MAP kinase and Akt pathways in oral squamous cell carcinoma by genistein and biochanin A. Evidence-Based Complementary and Alternative Medicine eCAM. 2010; 7:351–8. [PubMed: 18955325]
42. Widyarini S, Spinks N, Husband AJ, Reeve VE. Isoflavonoid compounds from red clover (Trifolium pratense) protect from inflammation and immune suppression induced by UV radiation. Photochemistry and Photobiology. 2001; 74:465–70. [PubMed: 11594062]
43. Nestel P, Cehun M, Chronopoulos A, DaSilva L, Teede H, McGrath B. A biochanin-enriched isoflavone from red clover lowers LDL cholesterol in men. European Journal of Clinical Nutrition. 2004; 58:403–8. [PubMed: 14985677]
44. Chen J, Miller EM, Gallo KA. MLK3 is critical for breast cancer cell migration and promotes a malignant phenotype in mammary epithelial cells. Oncogene. 2010; 29:4399–411. [PubMed: 20514022]
45. Khan AQ, Khan R, Rehman MU, Lateef A, Tahir M, Ali F, et al. Soy isoflavones (daidzein & genistein) inhibit 12-O-tetradecanoylphorbol-13-acetate (TPA)-induced cutaneous inflammation via modulation of COX-2 and NF-kappaB in Swiss albino mice. Toxicology. 2012; 302:266–74. [PubMed: 22981962]
46. Li YS, Wu LP, Li KH, Liu YP, Xiang R, Zhang SB, et al. Involvement of nuclear factor kappaB (NF-kappaB) in the downregulation of cyclooxygenase-2 (COX-2) by genistein in gastric cancer cells. The Journal of International Medical Research. 2011; 39:2141–50. [PubMed: 22289529]
47. Chadee DN, Xu D, Hung G, Andalibi A, Lim DJ, Luo Z, et al. Mixed-lineage kinase 3 regulates B-Raf through maintenance of the B-Raf/Raf-1 complex and inhibition by the NF2 tumor suppressor protein. Proceedings of the National Academy of Sciences of the United States of America. 2006; 103:4463–8. [PubMed: 16537381]
48. Chadee DN, Kyriakis JM. A novel role for mixed lineage kinase 3 (MLK3) in BRaf activation and cell proliferation. Cell Cycle (Georgetown Tex). 2004; 3:1227–9.
49. Shemesh M, Lindner HR, Ayalon N. Affinity of rabbit uterine oestradiol receptor for phyto-oestrogens and its use in a competitive protein-binding radioassay for plasma coumestrol. Journal of Reproduction and Fertility. 1972; 29:1–9. [PubMed: 5017011]

50. Harini R, Ezhumalai M, Pugalendi KV. Antihyperglycemic effect of biochanin A, a soy isoflavone, on streptozotocin-diabetic rats. European Journal of Pharmacology. 2012; 676:89–94. [PubMed: 22178203]

51. Shajib MT, Pedersen HA, Mortensen AG, Kudsk P, Fomsgaard IS. Phytotoxic effect, uptake, and transformation of biochanin A in selected weed species. Journal of Agricultural and Food Chemistry. 2012; 60:10715–22. [PubMed: 23030687]

52. Kole L, Giri B, Manna SK, Pal B, Ghosh S, Biochanin A. an isoflavon, showed anti-proliferative and anti-inflammatory activities through the inhibition of iNOS expression, p38-MAPK and ATF-2 phosphorylation and blocking NFkappaB nuclear translocation. European Journal of Pharmacology. 2011; 653:8–15. [PubMed: 21147093]

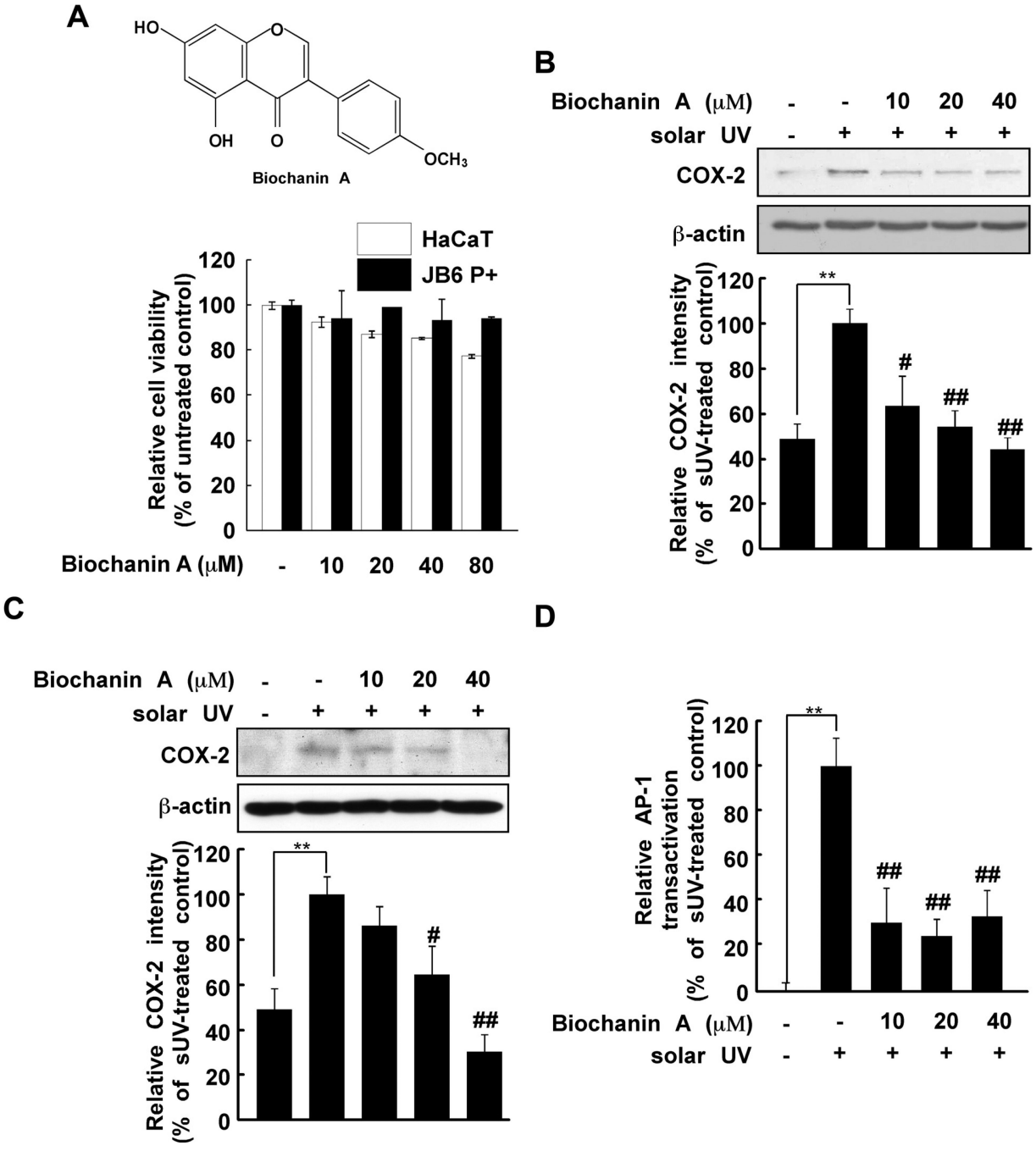

Fig. 1.

Effects of biochanin A on solar UV (sUV) induced cyclooxygenase (COX)-2 expression. (A) Chemical structure of biochanin (*upper*) and cytotoxicity of biochanin A against HaCaT and JB6 P+ cells (lower). The procedure for evaluating cytotoxicity is described in Section 2. (B) and (C) Biochanin A inhibits sUV-induced COX-2 expression in human HaCaT (B) and mouse JB6 P+ (C) cells. After treatment with biochanin A (0, 10, 20, or 40 μM) for 1 h, 2 the cells were irradiated with solar UV (sUV; 90 kJ/m^2) and harvested after 1 h. The protein levels of COX-2 and β-actin were measured by Western blotting. Data are

representative of 3 independent experiments that provided similar results. The level of β-actin was detected to verify equal loading of proteins. COX-2 expression was quantified using the Image J software program. (D) Biochanin A inhibits sUV-induced AP-1 transactivation in HaCaT cells. After treatment with biochanin A (0, 10, 20, or 40 μM) for 1 h, HaCaT cells transfected with an AP-1 luciferase plasmid were irradiated with sUV. Data are normalized to the transactivation of sUV-irradiated HaCaT cells (100%). The pound (# and ##) signs indicate significant differences at $p < 0.01$ and 0.001, respectively, compared to the sUV-treated group. The asterisks (**) indicate a significant induction of COX-2 (B, C) and AP-1 activity (D) induced by sUV. Representative blots from triplicate experiments with similar results are shown.

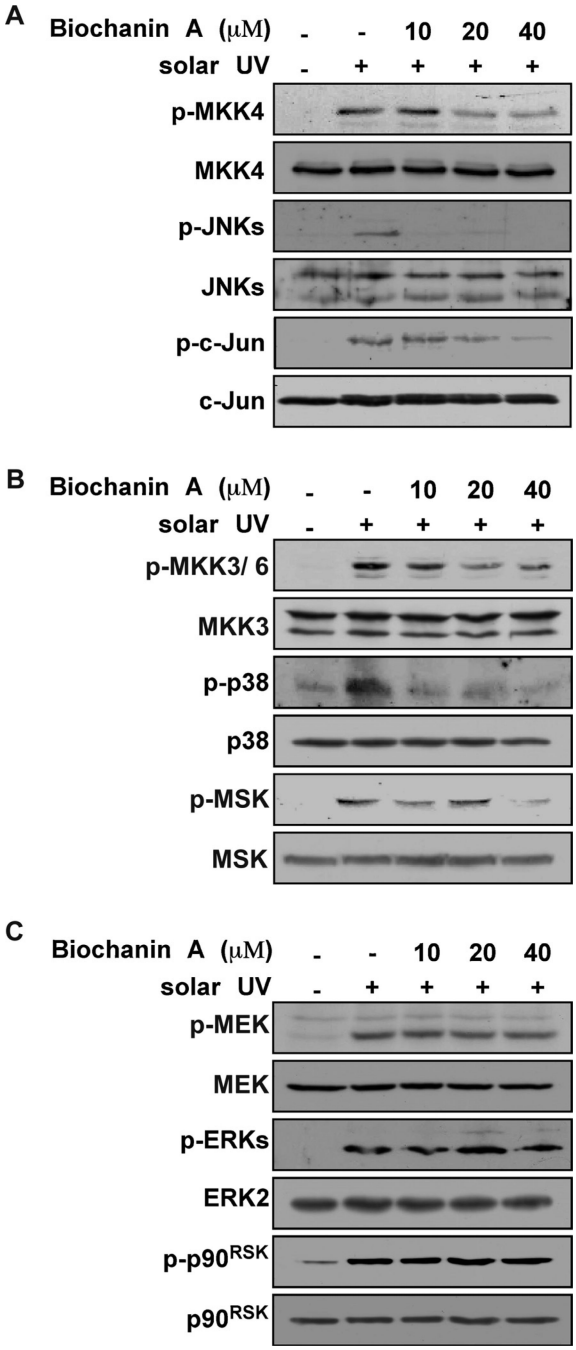

Fig. 2.

Effects of biochanin A on sUV-induced cellular signaling. (A)–(C) Biochanin A reduces sUV-induced MKK4/JNKs/c-Jun (A) and MKK3/6/p38/MSK (B) signaling, but not MEK/ERKs/p90RSK (C) signaling, in HaCaT cells. Cells were treated with biochanin A for 1 h, and then exposed to sUV. At 30 min after sUV irradiation, cells were collected and the phosphorylated and non-phosphorylated protein levels were determined by Western blotting. Representative blots from duplicate experiments with similar results are shown.

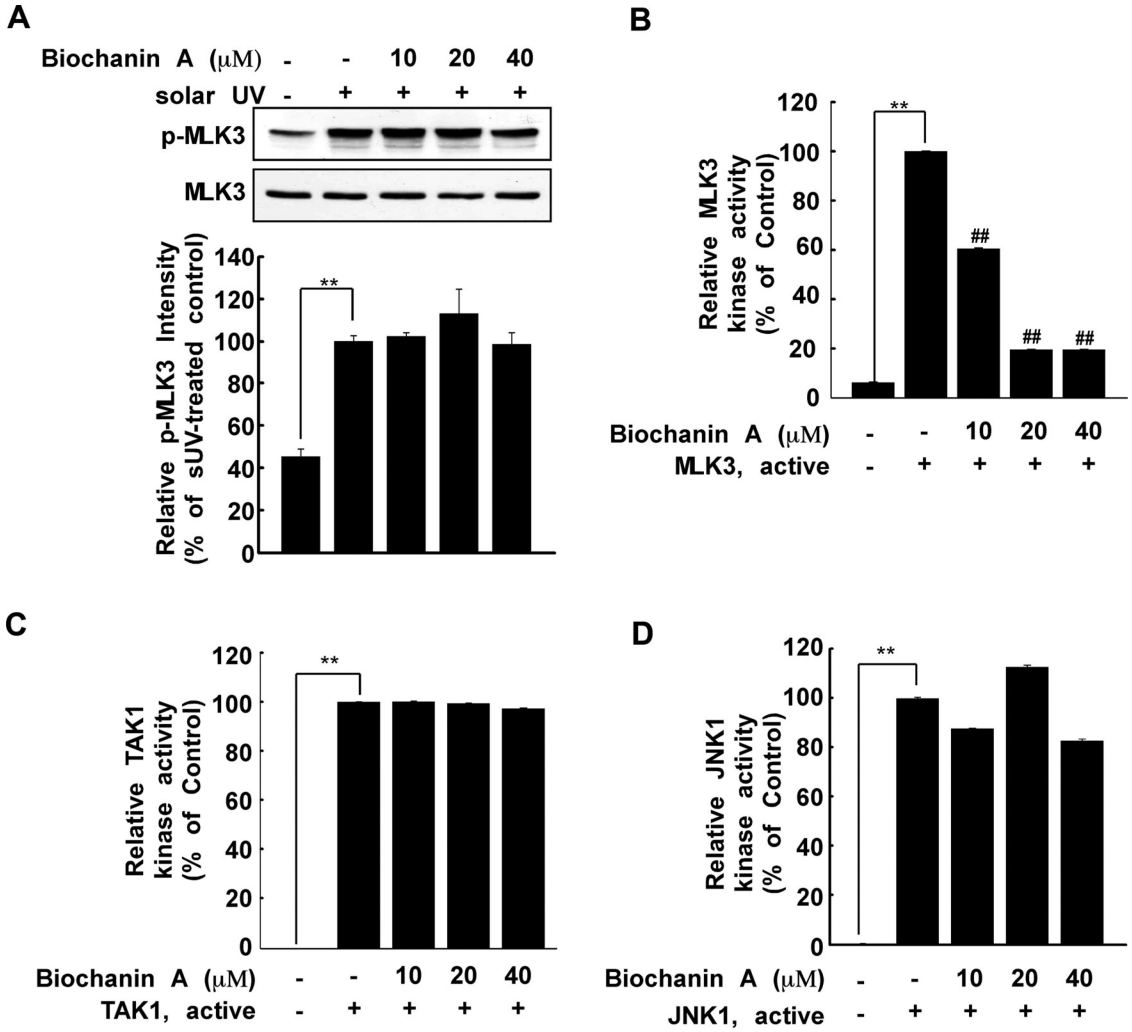

Fig. 3.

Biochanin A inhibits MLK3 kinase activity. (A) After treatment with biochanin A for 1 h, HaCaT cells were treated with sUV. The protein levels of phosphorylated and total MLK3 were measured by Western blotting. Phosphorylated MLK3 and total MLK3 were quantified using the Image J software program. (B) Biochanin A inhibits MLK3 kinase activity. Active MLK3 was incubated with biochanin A at the indicated concentrations for 15 min at 30 °C. MLK3 activity was measured as described in Section 2. (C) and (D) biochanin A does not affect TAK1 (C) or JNK1 (D) kinase activity. Active TAK1 or JNK1 (B) was incubated with biochanin A at the indicated concentrations for 15 min at 30 °C. Kinase activity was measured as described in Section 2. The asterisks (**) indicate a significant difference ($p < 0.001$) compared to untreated kinase control, and the pound symbols (##) indicate a significant difference ($p < 0.001$) compared to the untreated kinase control group.

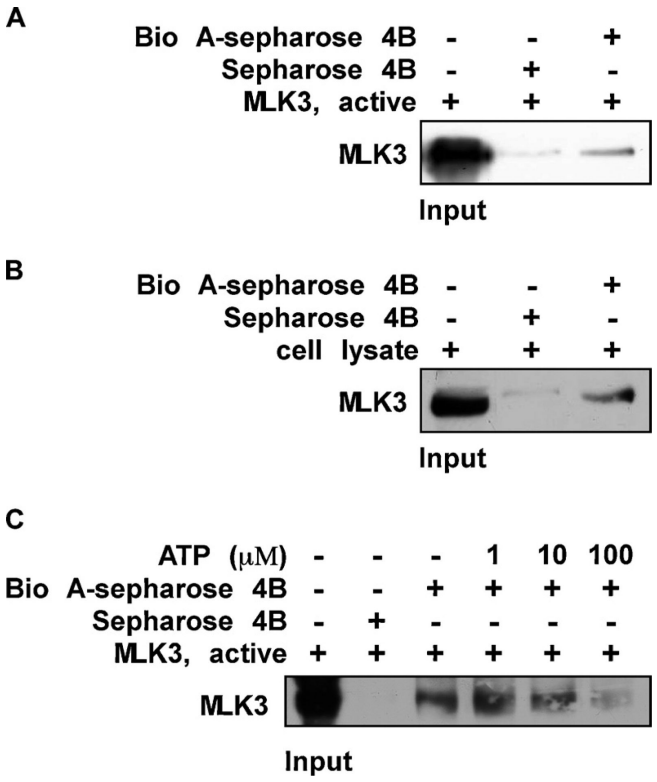

Fig 4.

Biochanin A directly binds to MLK3 in an ATP-competitive manner. (A) the MLK3-biochanin A binding *in vitro* was confirmed by immunoblotting using an antibody against MLK3; *first lane* (input control), MLK3 protein standards; *second lane* (control), Sepharose 4B used to pull down MLK3 as described in Section 2; *third lane*, MLK3 pulled down using biochanin A–Sepharose 4B affinity beads. (B) the MLK3-biochanin A binding *ex vivo* was investigated by immunoblotting using an antibody against MLK3; *first lane* (input control), whole-cell lysate from HaCaT cells; *second lane* (control), a lysate of HaCaT cells precipitated with Sepharose 4B beads as described in Section 2; *third lane*, whole-cell lysate from HaCaT cells precipitated by biochanin A–Sepharose 4B affinity beads as described in Section 2. (C) ATP at concentrations of 1, 10, or 100 μM was incubated with the MLK3 active protein for 1 h. Then the MLK3 protein was precipitated with biochanin A–Sepharose 4B affinity beads as described in Section 2. Representative blots from duplicate experiments with similar results are shown.

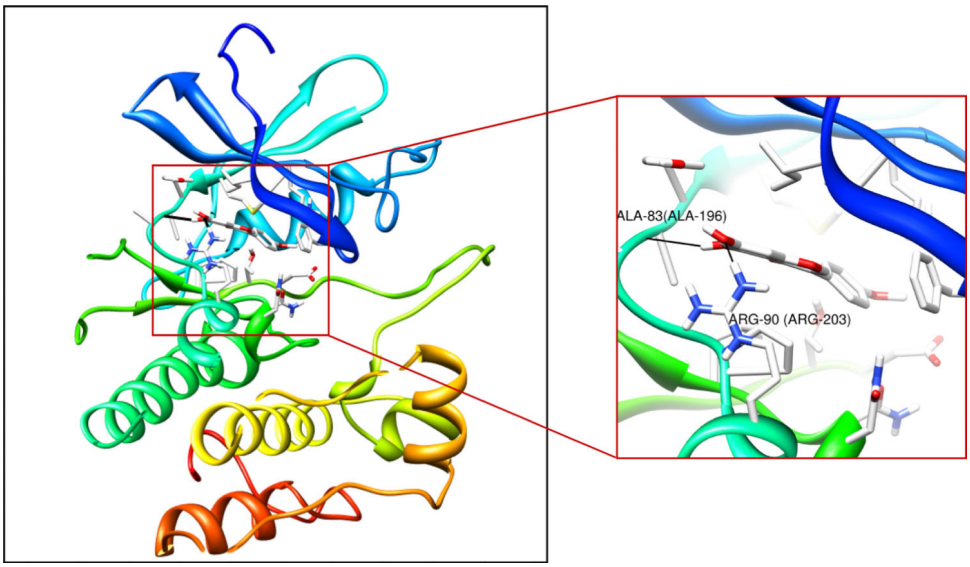

Fig. 5.

Binding mode of biochanin A with MLK3. Biochanin A is docked into the ATP-binding site of MLK3. Interaction of biochanin A with MLK3 (enlarged view). MLK3 is shown as a cartoon and side chains are shown as sticks. Biochanin A is shown in stick.

Table 1

Specificity of biochanin A against mitogen-activated kinase related kinases.

Kinase	Relative kinase activity (% of untreated control)
ASK1 (h)	103 ± 0
c-RAF (h)	86 ± 10
JNK1α1 (h)	98 ± 2
MAPK1 (h)	89 ± 4
MEK1 (h)	75 ± 7
MKK4 (m)	104 ± 3
MKK6 (h)	109 ± 5
MKK7β (h)	89 ± 6
MSK1 (h)	85 ± 5
PKBα (h)	101 ± 8
Rsk2 (h)	80 ± 5
SAPK2a (h)	88 ± 3
TAK1 (h)	91 ± 6
TAO1 (h)	80 ± 1
TAO2 (h)	84 ± 5